

Figure S1

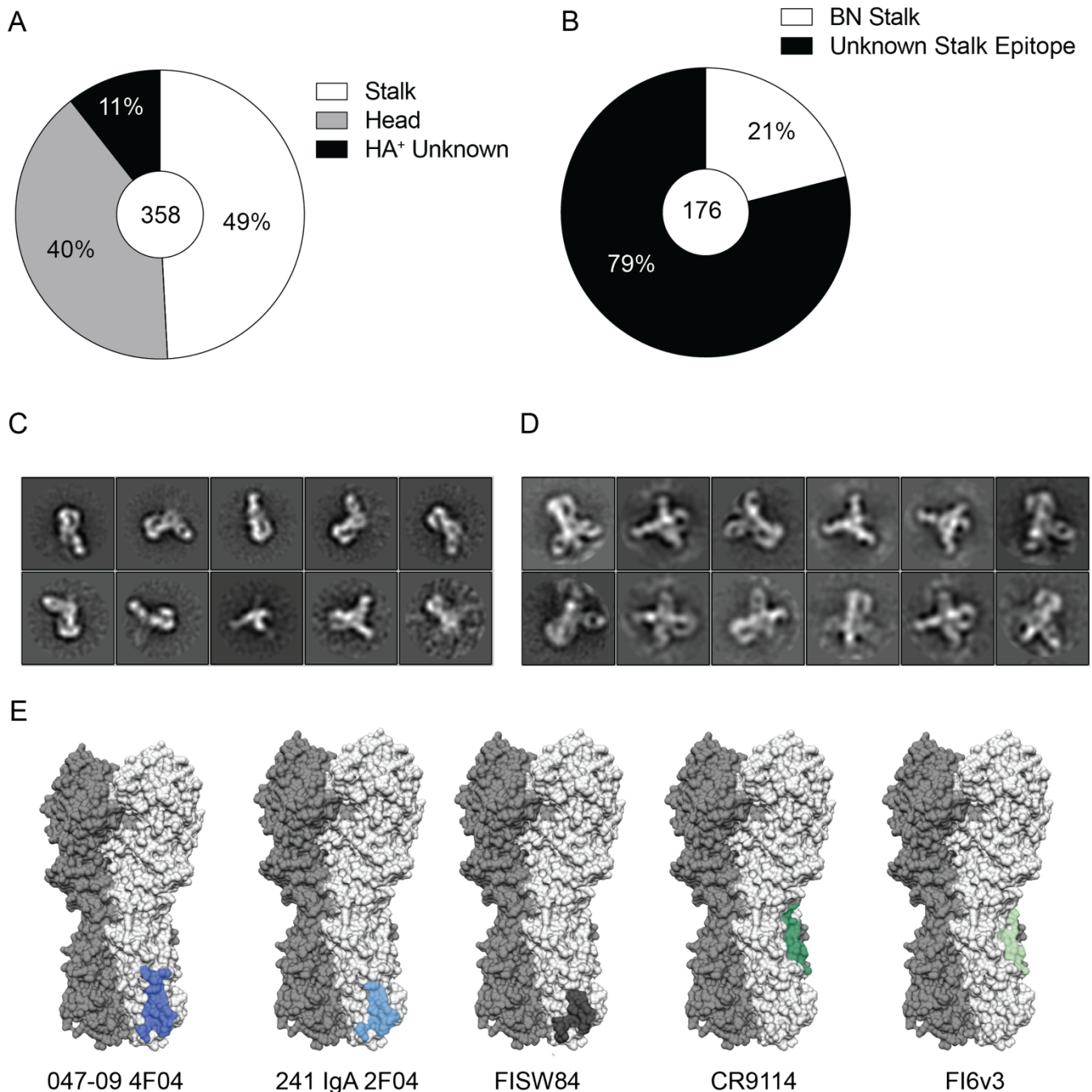


Figure S1: Binding features of isolated mAbs and 2D class average of anchor epitope binding mAbs. Related to Figure 1. (A) Proportion of HA⁺ mAbs binding to distinct HA domains. **(B)** Proportion of stalk-binding mAbs binding the BN stalk domain. **(C-D)** Negative stain 2D class averages of 047-09 4F04 **(C)** and 241 IgA 2F04 **(D)** binding A/California/4/2009 HA. **(E)** Binding footprint of mAbs binding the anchor epitope (047-09 4F04, 241 IgA 2F04, and FISW84) and the BN stalk epitope (CR9114 and FI6v3) on A/California/7/2009.

Figure S2

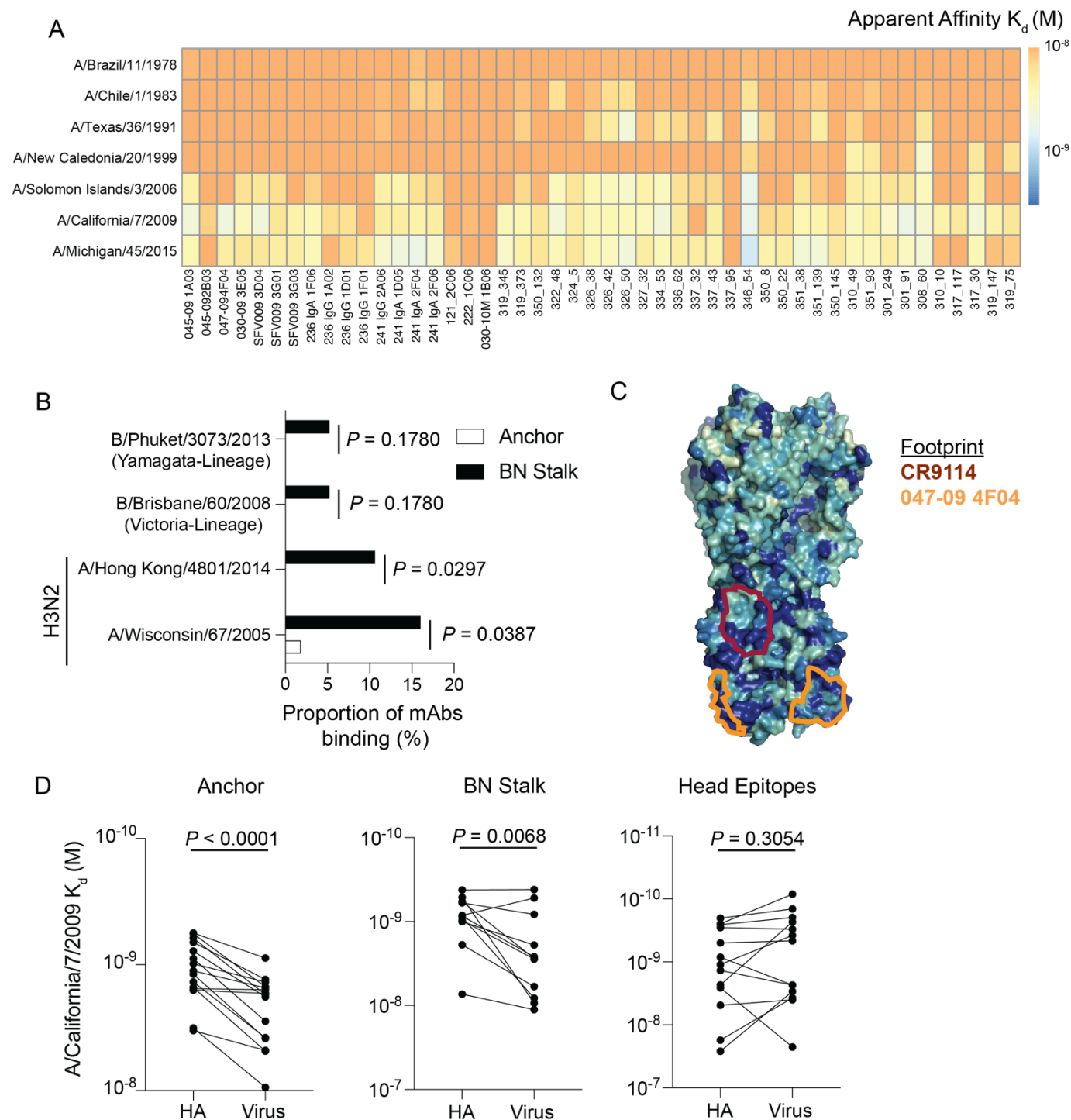


Figure S2: MAb targeted the anchor epitope binding to distinct H1N1 viruses, H3N2, influenza B viruses and comparison of mAbs binding virus versus HA. Related to Figure 2. (A) Heatmap of apparent affinity (K_d ; M) of anchor mAb binding to historical and recent H1N1 viruses. **(B)** Proportion of anchor binding and BN stalk binding mAbs binding to influenza B viruses and H3N2 viruses. **(C)** Conservation of group 1 influenza virus HAs, as shown on A/California/04/2009 (PDB: 4JTV), with the binding footprint of CR9114 (maroon) and 047-09 4F04 (orange) outlined. **(D)** Apparent affinity (K_d ; M) of mAbs binding anchor, BN stalk, or head epitope binding to recombinant HA from A/California/7/2009 H1N1 and A/California/7/2009 virus. Lines connect the same mAb. Data in **B** were analyzed by Fisher's Exact tests and data in **D** were analyzed using a paired non-parametric Wilcoxon matched-pairs signed rank test.

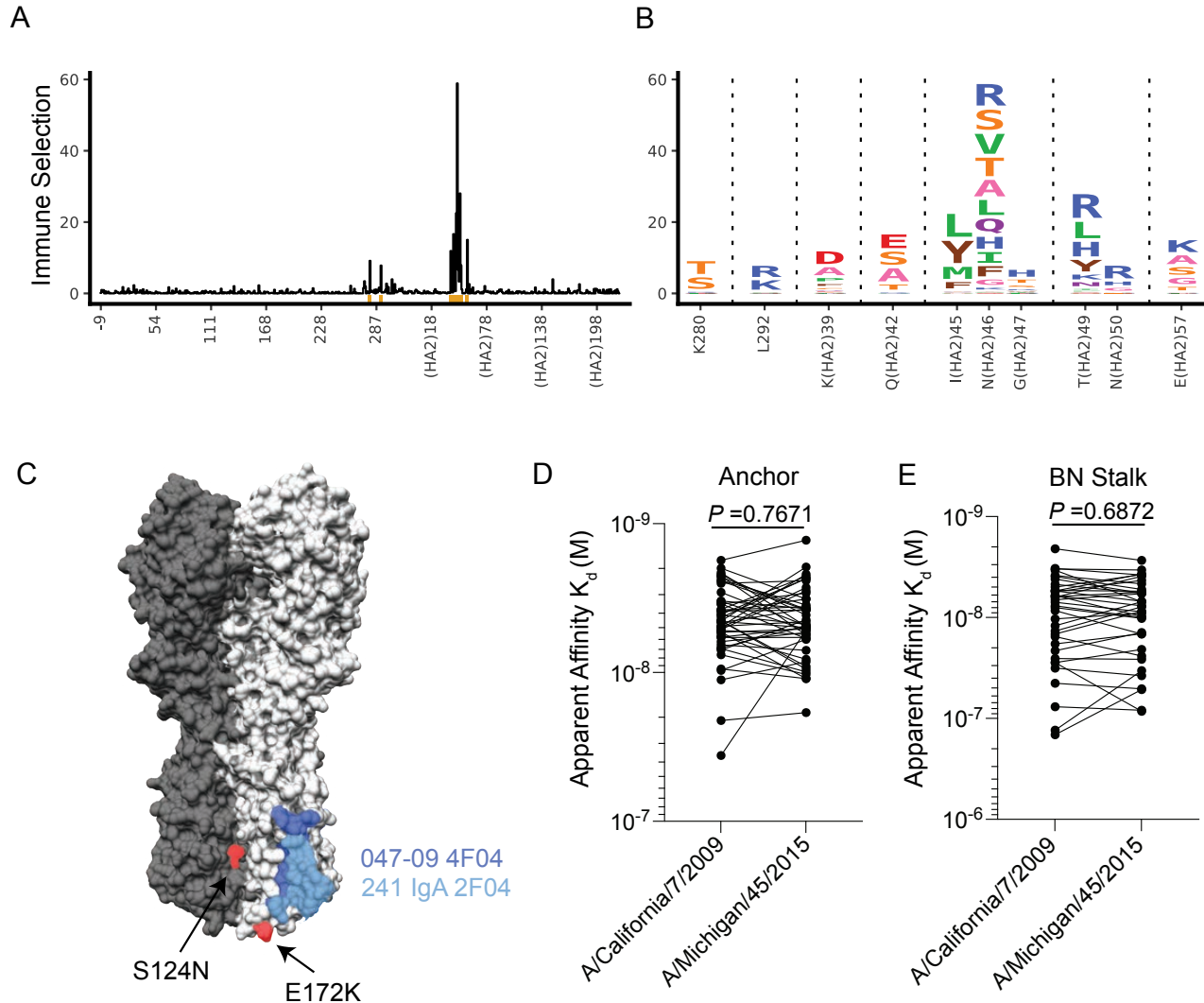


Figure S3: Deep mutational scanning of 045-09 2B06 and mAb affinity for A/Michigan/45/2015 H1N1. Related to Figure 2. (A-B) 045-09 2B06 was subjected to deep mutational scanning with a mutant library of A/WSN/1933 (H1N1). (A) Differential selection at each site in HA (H3 numbering). (B) Logo plot of key sites of escape, with the height of each letter proportional to the antibody selection for mutations to that amino acid at that site. (C) Differences in mutations found on the stalk domain of A/Michigan/45/2015 relative to the binding footprints of 047-09 4F04 and 241 IgA 2F04. (D-E) Apparent Affinity (K_d ; M) of anchor binding mAbs (D) and BN stalk binding mAbs (E) to A/California/7/2009 and A/Michigan/45/2009. Lines connect the same mAb. Data in D and E were analyzed using a paired non-parametric Wilcoxon matched-pairs signed rank test.

Figure S4

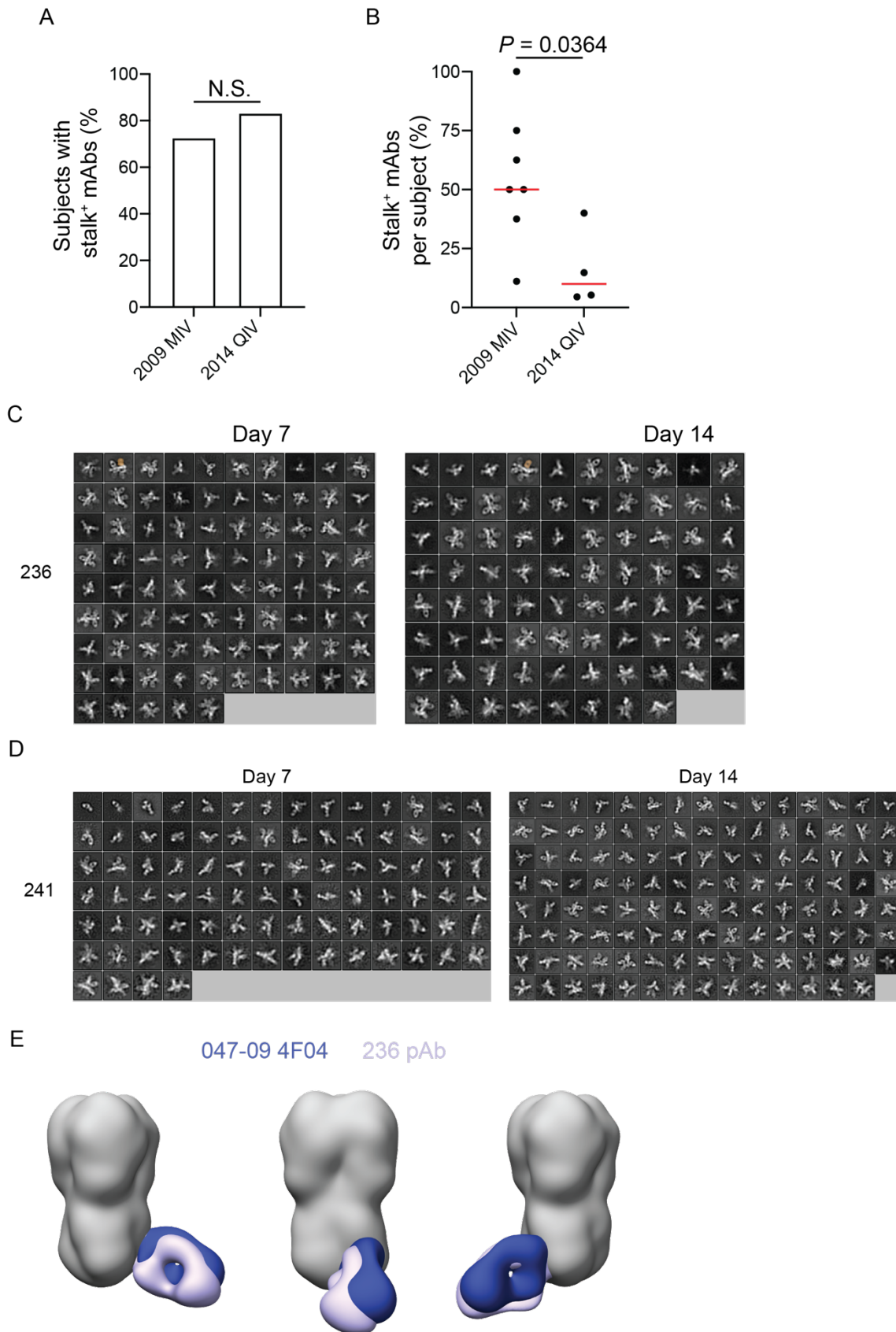


Figure S4: Characterization of stalk binding mAbs induced by influenza virus vaccines. Related to Figure 4. (A) Proportion of subjects with stalk⁺ mAbs from the 2009 MIV or 2014 QIV cohorts. (B) Proportion of mAbs targeting the stalk per person in the 2009 MIV and 2014 QIV cohorts. Red line represents the median. Each symbol in **B** represents one subject. Only subjects with stalk⁺ mAbs were included in the analysis. (C-D) 2D class averages of pAbs from subject 236 (C) and 241 (D) at days 7 and 14 post immunization binding to A/Michigan/45/2015 HA. (E) 3D reconstruction of the overlapping of 047-09 4F04, 236 pAb, and FISW84. Data in **A** were analyzed by Fisher's Exact tests and data in **B** were analyzed by unpaired non-parametric Mann-Whitney test.

Figure S5

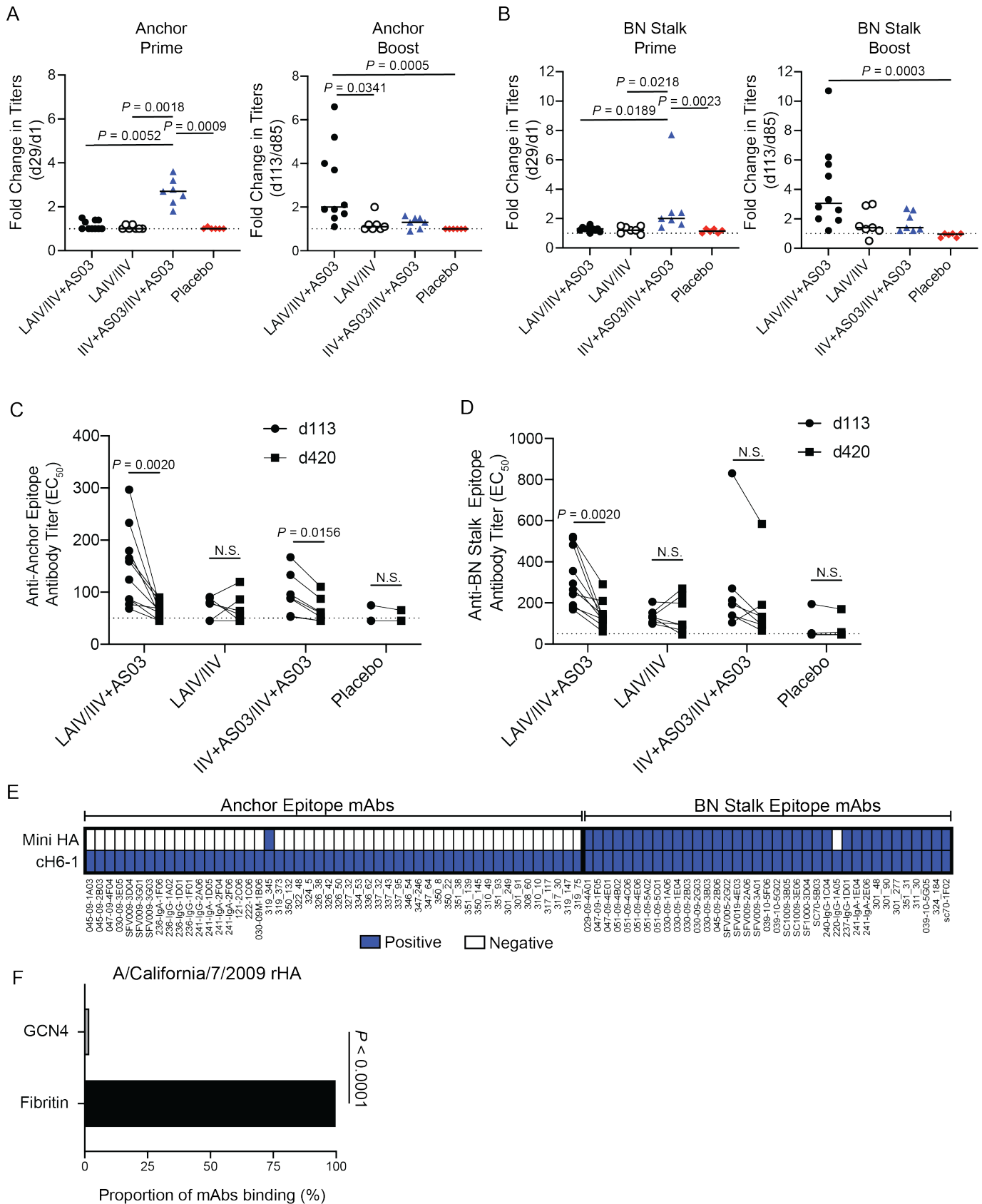


Figure S5: Seroconversion against anchor and BN stalk epitopes after cHA vaccination and mAb binding to various recombinant HAs. Related to Figure 5. (A-B) Seroconversion (d28/d0) of antibodies competing for binding against the anchor epitope (A) and the BN stalk epitope (B). Bar represents the

median and each symbol represents one subject. **(C-D)** Antibody titers (EC_{50}) of serum antibodies collected on day 112 and day 420 against the anchor epitope **(C)** and the BN stalk epitope **(D)**. Lines connect titers from the same subject and each pair of symbols represents one subject. **(E)** Anchor and BN stalk targeting mAbs binding to mini-HA and cH6/1. **(F)** Proportion of anchor epitope targeting mAbs binding to A/California/7/2009 recombinant HA with a GCN4 or fibritin trimerization domain. Data in **A** and **B** were analyzed by non-parametric Kruskal-Wallis Tests, data in **C** and **D** were analyzed using a paired non-parametric Wilcoxon matched-pairs signed rank test, and data in **F** were analyzed by a Fisher's Exact test.

Figure S6

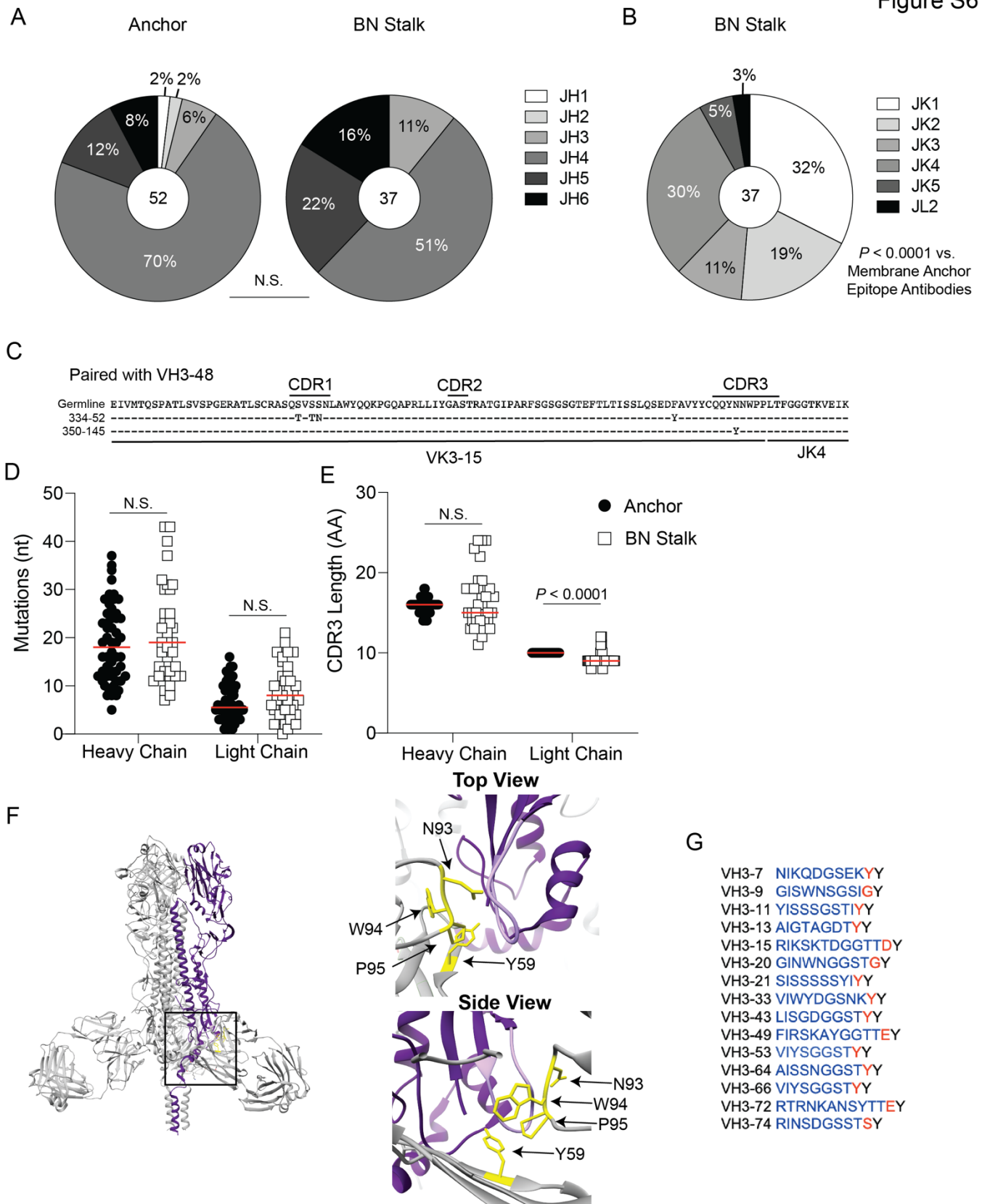


Figure S6: Additional repertoire features of mAbs binding the anchor epitope. Related to Figure 6. (A) JH gene usage by anchor and BN stalk binding antibodies. (B) JK gene usage of mAbs binding the BN stalk epitope. (C) VJ sequences of kappa chains of the public clone paired VH3-48. (D-E) Mutations (D) and CDR3 amino acid (AA) lengths (E) of heavy and light chains of mAbs binding the anchor or BN stalk

epitopes. Red bar represents median. **(F)** NWP motif of K-CDR3 and Y59 following H-CDR2 **(H)** of FISW84 (PDB: 6HJQ). **(G)** H-CDR2 sequences of germline VH3 genes. H-CDR2 is highlighted in blue and the first amino acid following H-CDR2 is highlighted in red. Data in **A** were analyzed using a Chi-square test, and data in **D** and **E** were analyzed by unpaired non-parametric Mann-Whitney tests.

Table S1: Subject information and demographics.

Subject	Vaccine/Infection	Age	Sex
029-09	2009 MIV	24	M
030-09	2009 MIV	31	F
045-09	2009 MIV	24	M
047-09	2009 MIV	22	M
051-09	2009 MIV	42	M
SFV005	2009 MIV	60	F
SFV009	2009 MIV	31	F
SFV015	2009 MIV	48	F
SFV018	2009 MIV	58	F
SFV019	2009 MIV	48	F
SFV020	2009 MIV	64	F
sc70	2009 pH1N1 Infection	38	F
sc1009	2009 pH1N1 Infection	21	M
SF1000	2009 pH1N1 Infection	37	M
008-10	2010 TIV	26	F
011-10	2010 TIV	30	M
014-10	2010 TIV	27	M
017-10	2010 TIV	24	M
019-10	2010 TIV	22	F
028-10	2010 TIV	38	M
034-10	2010 TIV	39	F
039-10	2010 TIV	25	M
051-10	2010 TIV	43	M
220-14	2014 QIV	24	F
221-14	2014 QIV	34	F
236-14	2014 QIV	32	F
237-14	2014 QIV	32	F
240-14	2014 QIV	28	M
241-14	2014 QIV	29	F
121/324 (d7/d112)	cHA – IIV+AS03/IIV+AS03	24	F
222/310 (d91/d112)	cHA – LAIV/IIV+AS03	25	F
301	cHA – IIV+AS03/IIV+AS03	34	F
308	cHA – LAIV/IIV+AS03	29	F
311	cHA – IIV+AS03/IIV+AS03	28	M
317	cHA – LAIV/IIV+AS03	37	M
319	cHA – LAIV/IIV+AS03	31	F
322	cHA – IIV+AS03/IIV+AS03	20	F
326	cHA – LAIV/IIV	27	M
327	cHA – LAIV/IIV+AS03	22	F
334	cHA – LAIV/IIV+AS03	33	M

336	cHA – LAIV/IIV+AS03	36	F
337	cHA – LAIV/IIV+AS03	27	F
346	cHA – LAIV/IIV	20	F
347	cHA – LAIV/IIV+AS03	31	F
350	cHA – LAIV/IIV+AS03	35	F
351	cHA – IIV+AS03/IIV+AS03	27	F

Table S2: Anchor epitope binding mAb information.

mAb	Cellular Source	VH	DH	JH	HC Clone #	VK	JK	KC Clone #
030-09 3E05	Plasmablast	3-23	3-22	4	Non-clonal	3-15	5	9
030-09M 1B06	MBC	3-23	3-10	4	Non-clonal	3-11	5	7
045-09 1A03	Plasmablast	3-23	6-13	4	Non-clonal	3-11	4	6
045-09 2B03	Plasmablast	3-23	5-12	4	Non-clonal	3-11	5	7
047-09 4F04	Plasmablast	3-48	6-19	4	Non-clonal	3-15	4	8
SFV009 3D04	Plasmablast	3-23	2-2	4	Non-clonal	3-15	4	8
SFV009 3G01	Plasmablast	3-30	3-16	4	Non-clonal	3-11	5	7
SFV009 3G03	Plasmablast	3-23	3-15-3	5	Non-clonal	3-11	5	7
236 IgG 1A02	Plasmablast	3-23	2-2	4	2	3-11	5	7
236 IgG 1D01	Plasmablast	3-23	6-19	4	Non-clonal	3-11	5	7
236 IgG 1F01	Plasmablast	3-23	2-2	4	2	3-11	5	7
236 IgA 1F06	Plasmablast	3-23	2-2	4	2	3-11	5	7
241 IgG 2A06	Plasmablast	3-23	6-19	5	Non-Clonal	3-15	4	8
241 IgA 1D05	Plasmablast	3-23	5-18	4	3	3-15	5	9
241 IgA 2F04	Plasmablast	3-23	2-21	4	3	3-15	5	9
241 IgA 2F06	Plasmablast	3-23	3-9	4	3	3-15	5	9
121 2C06	Plasmablast	3-23	2-15	4	Non-clonal	3-15	4	8
222 1C06	Plasmablast	3-48	2-15-2	4	Non-clonal	3-15	4	8
301_91	MBC	3-23	3-9	5	Non-clonal	3-11	5	7
301_249	MBC	3-48	5-24	3	Non-clonal	3-11	4	Non-clonal
301_275	MBC	3-23	2-21	4	1	3-15	4	8
308_60	MBC	3-23	1-26	4	Non-clonal	3-11	4	8
310_10	MBC	3-23	1-14	4	Non-clonal	3-15	4	8
310_49	MBC	3-23	3-22	4	Non-clonal	3-15	5	9
317_30	MBC	3-23	6-13	4	Non-clonal	3-15	4	8
317_117	MBC	3-23	2-2	4	Non-clonal	3-15	5	9
319_75	MBC	3-23	3-22	3	Non-clonal	3-11	5	7
319_147	MBC	3-48	3-15-3	6	Non-clonal	3-15	4	8
319_345	MBC	3-23	3-9	4	4	3-15	4	8
319_373	MBC	3-23	6-19	4	4	3-15	4	8
322_48	MBC	3-23	1-26	4	1	3-15	5	9
324_5	MBC	3-23	2-21	3	Non-clonal	3-15	5	9
326_38	MBC	3-23	1-26	4	Non-clonal	3-11	4	6
326_42	MBC	3-23	3-16	5	Non-clonal	3-15	4	8
326_50	MBC	3-30	5-12	4	Non-clonal	3-15	5	9
327_32	MBC	3-23	3-10	4	Non-clonal	3-15	4	8
334_52	MBC	3-48	6-13	6	5	3-15	4	8
334_53	MBC	3-23	2-2	4	Non-clonal	3-15	5	9
334_62	MBC	3-23	2-2	1	Non-clonal	3-11	4	6
337_32	MBC	3-30	5-24	4	Non-clonal	3-11	5	7
337_43	MBC	3-23	5-24	4	Non-clonal	3-15	4	8
337_95	MBC	3-48	3-16	6	Non-clonal	3-15	5	9
346_54	MBC	3-30-3	3-16	5	Non-clonal	3-11	4	6
347_64	MBC	3-23	1-7	2	Non-clonal	3-11	5	7
347_246	MBC	3-23	1-1	5	Non-clonal	3-15	5	9
350_8	MBC	3-23	3-16	4	Non-clonal	3-15	4	8
350_22	MBC	3-23	6-19	4	Non-clonal	3-11	4	6
350_132	MBC	3-48	1-26	4	Non-clonal	3-15	4	8
350_145	MBC	3-48	4-17	6	5	3-15	4	8
351_38	MBC	3-23	6-13	4	Non-clonal	3-15	4	8
351_93	MBC	3-23	1-1	4	Non-clonal	3-15	4	8
351_139	MBC	3-23	5-24	4	Non-clonal	3-11	4	6

Table S3: Mutation information for Figure 2C-D.

Mutation	Naturally Occurring?	045-09 2B06 Deep Mutational Scan?	Other Experimentally Determined?	Note	Source
H38S (HA1)		No	Yes	Affects C179 binding	(Doud et al., 2018)
L292R (HA1)		Yes		In footprint of many VH1-69 utilizing mAbs	(Lang et al., 2017)
I323V (HA1)	Yes	No		Present in pH1N1 viruses	(Xu et al., 2012)
K39D (HA2)		Yes	Yes	Contacts with VH3-30 mAb	(Fu et al., 2016)
Q42E (HA2)		Yes	Yes	Interact with CR9114 and FI6v3	(Wu et al., 2020)
A44V (HA2)		No	Yes	Expands in presence of stalk binding mAbs, escape mutant of 6F12	(Park et al., 2020; Tan et al., 2012)
I45L (HA2)		Yes	Yes	Mutation associated with resistance to group 1 neutralizing stalk mAbs	(Lingwood et al., 2012; Wu et al., 2020; Yassine et al., 2018)
D46R (HA2)		Yes		Pre-pH1N1 viruses express N46	
E47K (HA2)	Yes	Yes		Associated with HA protein stability	(Cotter et al., 2014)
T49R (HA2)		Yes		Mutation associated with resistance to group 1 neutralizing stalk mAbs	(Lingwood et al., 2012; Yassine et al., 2018)
N50R (HA2)		Yes		Interacts with CR9114	(Dreyfus et al., 2012)
V52A (HA2)		No	Yes	Affects FI6v3 mAb binding	(Wu et al., 2020)
I56A (HA2)		No	Yes	Affects F10 mAb binding	(Sui et al., 2009)
E57K (HA2)		Yes		Critical residue for membrane fusion	(Vanderlinden et al., 2010)

Table S4: MAbs used in Figure 3 infection studies.

mAb name	Epitope Specificity
241 IgG 2A06	Anchor
047-09 4F04	Anchor
030-09 3E05	Anchor
SFV009 3G01	Anchor
236 IgG 1A02	Anchor
045-09 2B06	BN Stalk
SFV005 2G02	BN Stalk
SFV019 4E03	BN Stalk
220 IgG 1A05	BN Stalk
241 IgA 2E06	BN Stalk

Table S5: Group 1 HA strains used in Fig. S2C.

HA Subtype	Strain Name
H1	A/California/04/2009
H2	A/Singapore/1/1957
H5	A/mallard/Italy/3401/2005
H6	A/chicken/Taiwan/0705/1999
H8	A/turkey/Ontario/6118/1968
H9	A/swine/HongKong/9/1998
H11	A/duck/England/1/1956
H12	A/duck/Alberta/60/1976
H13	A/gull/Maryland/704/1977
H16	A/black-headed-gull/Turkmenistan/13/1976
H17	A/little-yellow-shouldered-bat/Guatemala/060/2010
H18	A/flat-facedbat/Peru/033/2010

References

- Cotter, C.R., Jin, H., and Chen, Z. (2014). A single amino acid in the stalk region of the H1N1pdm influenza virus HA protein affects viral fusion, stability and infectivity. *PLoS Pathog* *10*, e1003831.
- Doud, M.B., Lee, J.M., and Bloom, J.D. (2018). How single mutations affect viral escape from broad and narrow antibodies to H1 influenza hemagglutinin. *Nat Commun* *9*, 1386.
- Dreyfus, C., Laursen, N.S., Kwaks, T., Zuijdgeest, D., Khayat, R., Ekiert, D.C., Lee, J.H., Metlagel, Z., Bujny, M.V., Jongeneelen, M., *et al.* (2012). Highly conserved protective epitopes on influenza B viruses. *Science* *337*, 1343-1348.
- Fu, Y., Zhang, Z., Sheehan, J., Avnir, Y., Ridenour, C., Sachnik, T., Sun, J., Hossain, M.J., Chen, L.M., Zhu, Q., *et al.* (2016). A broadly neutralizing anti-influenza antibody reveals ongoing capacity of haemagglutinin-specific memory B cells to evolve. *Nat Commun* *7*, 12780.
- Lang, S., Xie, J., Zhu, X., Wu, N.C., Lerner, R.A., and Wilson, I.A. (2017). Antibody 27F3 Broadly Targets Influenza A Group 1 and 2 Hemagglutinins through a Further Variation in VH1-69 Antibody Orientation on the HA Stem. *Cell Rep* *20*, 2935-2943.
- Lingwood, D., McTamney, P.M., Yassine, H.M., Whittle, J.R., Guo, X., Boyington, J.C., Wei, C.J., and Nabel, G.J. (2012). Structural and genetic basis for development of broadly neutralizing influenza antibodies. *Nature* *489*, 566-570.
- Park, J.K., Xiao, Y., Ramuta, M.D., Rosas, L.A., Fong, S., Matthews, A.M., Freeman, A.D., Gouzoulis, M.A., Batchenkova, N.A., Yang, X., *et al.* (2020). Pre-existing immunity to influenza virus hemagglutinin stalk might drive selection for antibody-escape mutant viruses in a human challenge model. *Nat Med* *26*, 1240-1246.
- Sui, J., Hwang, W.C., Perez, S., Wei, G., Aird, D., Chen, L.M., Santelli, E., Stec, B., Cadwell, G., Ali, M., *et al.* (2009). Structural and functional bases for broad-spectrum neutralization of avian and human influenza A viruses. *Nat Struct Mol Biol* *16*, 265-273.
- Tan, G.S., Krammer, F., Eggink, D., Kongchanagul, A., Moran, T.M., and Palese, P. (2012). A pan-H1 anti-hemagglutinin monoclonal antibody with potent broad-spectrum efficacy in vivo. *J Virol* *86*, 6179-6188.
- Vanderlinden, E., Goktas, F., Cesur, Z., Froeyen, M., Reed, M.L., Russell, C.J., Cesur, N., and Naesens, L. (2010). Novel inhibitors of influenza virus fusion: structure-activity relationship and interaction with the viral hemagglutinin. *J Virol* *84*, 4277-4288.
- Wu, N.C., Thompson, A.J., Lee, J.M., Su, W., Arlian, B.M., Xie, J., Lerner, R.A., Yen, H.L., Bloom, J.D., and Wilson, I.A. (2020). Different genetic barriers for resistance to HA stem antibodies in influenza H3 and H1 viruses. *Science* *368*, 1335-1340.
- Xu, R., Zhu, X., McBride, R., Nycholat, C.M., Yu, W., Paulson, J.C., and Wilson, I.A. (2012). Functional balance of the hemagglutinin and neuraminidase activities accompanies the emergence of the 2009 H1N1 influenza pandemic. *J Virol* *86*, 9221-9232.
- Yassine, H.M., McTamney, P.M., Boyington, J.C., Ruckwardt, T.J., Crank, M.C., Smatti, M.K., Ledgerwood, J.E., and Graham, B.S. (2018). Use of Hemagglutinin Stem Probes Demonstrate Prevalence of Broadly Reactive Group 1 Influenza Antibodies in Human Sera. *Sci Rep* *8*, 8628.